ELSEVIER

Chemical Engineering Journal 68 (1997) 75–86

Chemical Engineering Journal

Local measurements of fluid and particle velocities in a stirred suspension

P. Guiraud *, J. Costes, J. Bertrand

Laboratoire de Génie Chimique — UMR 5503 CNRS Ecole Nationale Supérieure d'Ingénieurs de Génie Chimique 18, Chemin de la Loge, F-31078 Toulouse Cedex 4, France

Received 5 May 1996; accepted 4 March 1997

Abstract

An experimental approach is proposed for the measurement of the local behaviour of continuous and dispersed phases in a stirred suspension at low particle concentrations (0.5 vol.%). The basic principle involves the simultaneous measurement of the local velocity and particle size with a phase Doppler velocimeter and the separation of the data obtained from large particles (representing the dispersed phase) and very small particles (representing the motion of the continuous liquid phase).

This technique was applied to the investigation of a fully baffled cylindrical vessel, with a flat bottom, stirred by an industrial axial propeller. The diameters of the vessel and the propeller and the vertical clearance were 0.3 m, 0.14 m and 0.1 m respectively. The liquid was water and spherical glass particles were used as the dispersed phase.

In the absence of particles, the circulation pattern created by the propeller in the middle plane between two baffles revealed a major circulation loop in the lower part of the vessel and a minor contra-rotative loop in the wall surface corner. The calculated pumping coefficient, circulation flow number, non-dimensional time of renewal and circulation time were 0.62, 0.89, 11.76 and 8.15 respectively. The tangential velocities remained at values of less than 15% of the impeller tip velocity in the plane of the measurements.

Axial, radial and tangential mean and root-mean-square velocities for the carrier liquid phase and particles were measured in the two-phase flow, using particles with a mean diameter of 253 μm. These measurements showed that the particles lagged behind the liquid phase in the upward parts of the flow field, but were ahead in some downward parts. The root-mean-square axial velocities obtained for the particles were always greater than these obtained for the continuous phase. Non-homogeneities in the suspension were observed by the local mean diameter field. The effects of the stirring rate and size of the particles were also checked in the upward part of the flow in the vessel. © 1997 Elsevier Science S.A.

Keywords: Stirred tank reactors; Particle suspension; Phase Doppler technique; Local velocities

1. Introduction

Mechanical agitation is widely used in the chemical, food and pharmaceutical industries for operations such as blending, heat transfer, mass transfer, chemical reaction, etc. Various processes involving two-phase solid–liquid flows can be performed in a stirred tank: promotion of a chemical reaction between two phases; promotion of dissolution or crystal growth; achievement of a uniform particle concentration (and/or size distribution) in a stream [1].

The local characteristics of a stirred suspension are very important, because they are involved in many phenomena, such as attrition in crystallizers, and an efficient design of a stirred tank requires an understanding of the fluid mechanics within the vessel.

Single-phase turbulent flow characteristics in stirred tanks have been investigated in many experimental studies by laser Doppler velocimetry [2–6]. A number of numerical predictions have been devoted to the description of the local turbulent velocity field within two-dimensional (2D) [7] or three-dimensional (3D) [8,9] domains.

Studies of two-phase stirred suspensions have mainly dealt with the overall performance of equipment: power consumption; mass transfer rates between the liquid and particles [10]; description of scale-up criteria; determination of the critical agitator speed to ensure the suspension of particles. A review of such results has been made by Gray and Oldshue [11]. Most investigations devoted to local measurements have dealt with the axial solid concentration profiles [12–14]. Only a few studies have investigated the local measurements of hydrodynamics in suspensions. This situation is certainly due to the difficulty of finding a suitable measurement technique for such two-phase systems. Geisler and Mersmann [15]

* Corresponding author. Tel: (33) 05 62 25 23 75. Fax: (33) 05 62 25 23 18. E-mail: Pascal.Guiraud@ensigct.fr

PII S1385-8947(97)00076-4

have measured the mean and root-mean-square velocities of a continuous liquid phase in a tank equipped with a marine-type propeller by adjusting the refractive index of the fluid mixture to that of the glass particles. They compared these measurements with others performed in a single-phase flow, and showed that the velocity and turbulence fields present in a stirred suspension were different from those encountered in a single-phase flow. Nouri and Whitelaw [16] have also matched the refractive index of their continuous phase with that of dispersed particles, but devoted their measurements to the behaviour of the particles. Their results also demonstrated the considerable influence of the presence of the particles on the flow field, even when the volumetric concentration was very low (about 0.02%).

The aim of this study is to apply a new experimental method to the measurement of local characteristics in suspensions. Firstly, the basis of this technique is explained. The experimental equipment is then described. The final section presents the results obtained in a fully baffled cylindrical vessel, equipped with an industrial axial propeller.

2. Local measurements in liquid–solid suspensions

The objective of this work was to obtain the local velocities of the continuous liquid flow and dispersed phase (particles) suspended in a stirred vessel. The use of an intrusive measurement technique is prohibited in such systems, because the probes are often larger than the particles and disturb the flow [17]. A number of non-intrusive methods for the measurement of particle velocities have been developed in the last decade: transit time or correlation techniques; laser transit velocimetry (LTV) [18]; particle image velocimetry (PIV); particle tracking velocimetry [19]; laser speckle velocimetry [20]; Doppler techniques. Of these methods of measurement, the first does not enable the determination of the sign of the velocity, and therefore the technique is prohibited in turbulent flows such as stirred suspensions. The second and third methods use high speed cinematography, pulsed lasers, laser analysis of pictures, etc. They require very expensive equipment, considerable experience in this type of measurement and are very difficult to apply in 3D flows. Doppler techniques are well known and clearly measure the velocity of particles.

Laser Doppler velocimetry seems to be the ideal basic technique to build a suitable experimental method to measure the velocities of the continuous and dispersed phases in a suspension. The basic idea involves the separation of the data obtained from large particles (dispersed phase) and very small particles (representing the motion of the continuous liquid phase with the same velocity) (this assumption is always applied in laser Doppler velocimetry).

Although several methods for carrying out this discrimination of the Doppler signals exist, commercial equipment is not available when a calibration is necessary at each measurement point. For instance, some methods are based on amplitude discrimination of the Doppler bursts occurring when particles cross the measurement volume. This amplitude is a function of the particle size [21,22]. The main problem of these methods lies in the fact that amplitude measurements of a light signal are dependent on a number of optical elements, particularly when the flow is confined by walls (the tank); calibration must be performed at each measurement point, and the measurement conditions can evolve during an experiment because of fouling.

A more interesting method of discrimination of the signals obtained from small and large particles is based on the frequency of the Doppler burst. This technique uses the phase difference between the Doppler signals (obtained from a particle crossing the measurement volume) received by two photomultipliers directed towards the measurement volume at different angles. The phase difference is a function of the particle size [23]. The velocity and size of each particle crossing the measurement volume can be measured and stored. After data analysis, the velocity of the continuous phase (liquid) can be deduced from the smallest particles in the flow; the velocity and size distribution of the dispersed phase are deduced from the other particles. This technique has been chosen in this work for several reasons: it is a eulerian non-intrusive technique; the validity of the velocity measurements has been checked in several flows; the size measurements do not need calibration; equipment is now commercially available. However, this technique provides no information on the phase fraction distribution.

3. The phase Doppler size and velocity measurement technique

Ten years after the work carried out by Durst and Zare [23], the first papers on the phase Doppler equipment were published by Bachalo and Houser [24], Bauckage and Floegel [25] and Saffman et al. [26].

As in the well-known laser Doppler velocimetry (LDV), the phase Doppler technique uses two laser beams focused to obtain a beam intersection. In this intersection, planar interference fringes are produced parallel to each other and separated by a distance known as the fringe spacing δ

$$\delta = \lambda_0 (2 \sin \theta/2) \quad (1)$$

where λ_0 is the wavelength of the laser and θ is the intersection angle between the laser beams.

Although LDV measurements require only one photomultiplier to detect the Doppler frequency of the light scattered by a particle passing the fringes, the phase Doppler technique needs a second (Fig. 1) in order to detect the Doppler burst, but with a typical time difference relating to the particle velocity and to the curvature of its surface (the diameter of a spherical particle).

The velocity V of the particle can be deduced from the Doppler frequency F_d measured by a counter by the relation [2]

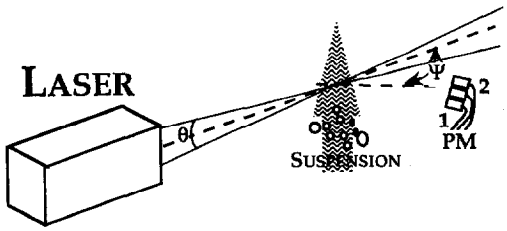

Fig. 1. Phase Doppler measurement system.

$$V = F_d \delta \quad (2)$$

The time difference Δt (Fig. 2) can be expressed as a phase difference Φ by the relation [3]

$$\Phi = F_d \Delta t \quad (3)$$

Φ can be correlated with the diameter d of spherical particles by the following equation [24,25]

$$d = \Phi / 2b(\lambda_0 / \pi n_l) \quad (4)$$

where n_l is the refractive index of the liquid phase and b is a function of the geometrical arrangement of the experimental set-up.

The dependence of Φ vs. d is linear in certain special cases and when the off-axis angle Ψ (Fig. 1) is well chosen. The linearity in this special case has been computed using Mie theory or geometrical optic laws [27] and has been checked experimentally [24]. In commercially available equipment, three detectors are used to improve the accuracy and range of the size measurements.

For each particle crossing the measurement volume, the Doppler frequency and phase difference are measured, and the velocity and diameter are stored on a personal computer. Data analysis is performed off-line and provides size and velocity distributions, as well as the size–velocity correlation, useful for discriminating between the velocity of large (dispersed phase) and small (representing the continuous phase) particles. It is very difficult to obtain a sufficient number of data for each category of particles (small and large) when only one measurement is performed over a wide size range (from a few micrometres to 400 μm). In order to obtain a more accurate value of the mean and root-mean-square velocities of each phase, two measurements are performed successively at every point by modifying the intersection angle θ between the incident laser beams and, consequently, the size range of the measurements. At each measurement point, the mean and root-mean-square velocities are extracted from 1000 and 10 000 particles for the continuous and dispersed phases respectively.

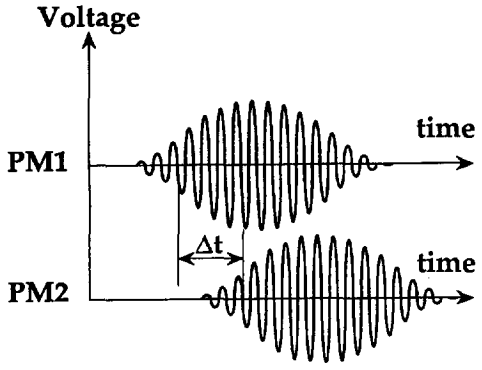

Fig. 2. Time difference between bursts at two photomultipliers.

4. Experimental equipment and instrumentation

The mixing tank (Fig. 3) is a fully baffled cylindrical vessel consisting of an acrylic transparent cylinder with an inside diameter T of 0.3 m, with a flat bottom. Four acrylic baffles of width $B_w = T/10$ are located along the vessel periphery. The vessel is placed in a square glass tank, filled with water, in order to obtain known deflections of the laser beams, and to reduce the problems associated with refraction by the curved surface.

The height H of the suspension in the tank is equal to its diameter T (0.3 m). The volume of the vessel is approximately 0.021 m^3. The suspension is obtained via an industrial propeller (Mixel TT), the diameter D of which is 0.14 m ($D/T = 0.47$). The impeller clearance C and the diameter of the vessel are in the ratio 1:3. The height h of the propeller is 34×10^{-3} m. The thicknesses of the blades and baffles are 2×10^{-3} m and 5×10^{-3} m respectively, and the shaft diameter is 25×10^{-3} m.

As is usual in stirred tank studies, the origin of the cylindrical coordinates is taken on the axis of the vessel at the stirrer level, the diameter D of which is the reference length. As a consequence, the dimensionless radial coordinate r/D varies between zero (on the axis of the vessel) and 0.94 (on the wall) and the edge of the impeller is located at $r/D = 0.5$.

The continuous phase is water. For the dispersed phase, spherical glass particles have been chosen (density, 2.23×10^3 kg m^{-3}). Their size distribution has been measured with a laser light scattering Malvern Sizer 2600. The mean volume diameter is 253 μm. The size distribution is reported in Table 1.

The volumetric concentration of the solid phase is 0.5%, so that the apparent viscosity of the suspension is similar to

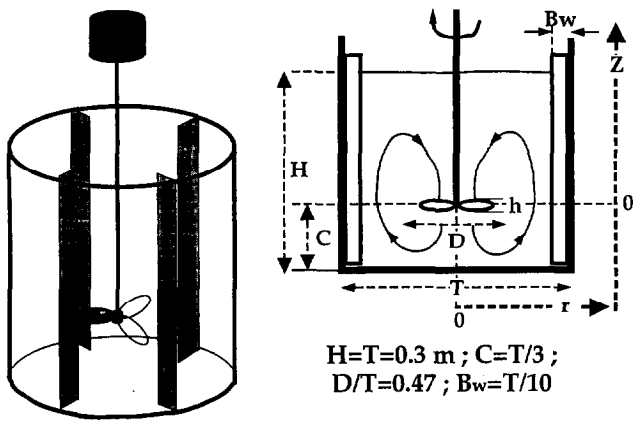

Fig. 3. The mixing vessel.

Table 1
Size distribution of the solid phase (Malvern Sizer 2600)

Size (μm)	Vol.% in band
>346	0
299–346	17.2
258–299	28.6
222–258	29.0
192–222	18.4
165–192	5.8
<165	1

the water viscosity. It is assumed that the viscosity is not affected by the presence of particles.

A phase Doppler particle analyser (AEROMETRICS PDPA 100) is used to measure the velocity and size of the particles. A 10 mW He–Ne laser is used as the light source. It is followed by a 3× beam expander, a beam splitter and a focusing lens. The receiver consists of a lens located at an off-axis angle Ψ of 30° with the plane of the incident beams, with a pinhole focusing on three photodetectors. The signals from the photodetectors are amplified and transferred to a counter-type processor. The size and velocity are stored via direct memory access in approximately 20 μs to a COMPAQ DESKPRO 386/20 personal computer.

In order to measure the size of the particles, the relative positions of the emitter and receiver must be held (in particular the off-axis angle) when the measurement point is moved over the volume of the tank. Each part of the apparatus is mounted on a traversing system which enables six degrees of freedom to be attained: four translations and two rotations.

Measurements are performed in the vessel on a vertical plane located at a middle angular position between two baffles. A special arrangement of the emitter and receiver is necessary for each velocity component to be measured to maintain the off-axis angle Ψ at a constant value of 30° which is necessary in the case of a water–glass particle system. The three arrangements are presented in Fig. 4(a)–4(c) for the measurement of the axial, radial and tangential velocity components respectively. It should be noted that the measurement of the tangential component is only possible under the propeller if the sizes of the particles are determined at the same time.

All the velocities have been normalized to the impeller tip speed πND, and the axial and radial distances to the impeller diameter D.

The impeller speed N is 5.1 s^{-1}; the Reynolds number Re and the impeller tip velocity V_t are 10^5 and 2.24 m s^{-1} respectively with

$$\mathrm{Re} = ND^2/\nu \tag{5}$$

5. The velocity field in a single-phase flow

A preliminary investigation of the flow field has been performed in the absence of particles in order to obtain reference data for comparison with measurements in a two-phase situation, and to draw up a map of the velocity field for the calculation of the characteristic numbers of this propeller-tank situation [3].

These measurements, carried out on a mesh of 14×30 points, are reported in Fig. 5. This map shows, by arrows, the combination of the axial and radial dimensionless components of the mean velocity. The circulation pattern confirms the classification of this industrial propeller as an axial flow type: the radial velocity component remains very slight under the propeller. The discharge flow issuing from the propeller impacts on the wall bottom, creating an important radial flow parallel to the bottom which impinges on the cylindrical walls of the vessel. In this way, the corner of the tank diverts the flow upwards, creating an important circulation loop at the level of the propeller. The mean velocity values are small in the upper part of the vessel, because of the low position ($C/T = 1/3$) of the propeller. A small contra-rotative circulation loop can be observed along the wall of the tank near the free surface of the liquid; it creates downward velocities near the wall up to $Z/D = 0.6$.

The pumping capacity Q_p can be determined from the discharge flow of the propeller

$$Q_p = -2\pi \int_0^{D/2} V_z\, r\, \mathrm{d}r \tag{6}$$

The pumping coefficient N_{Q_p} of the propeller is then deduced

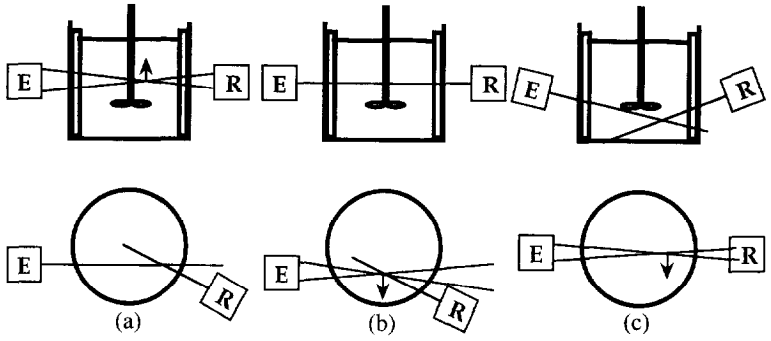

Fig. 4. Emitter (E) and receiver (R) arrangements to measure (a) axial velocity, (b) radial velocity, (c) tangential velocity.

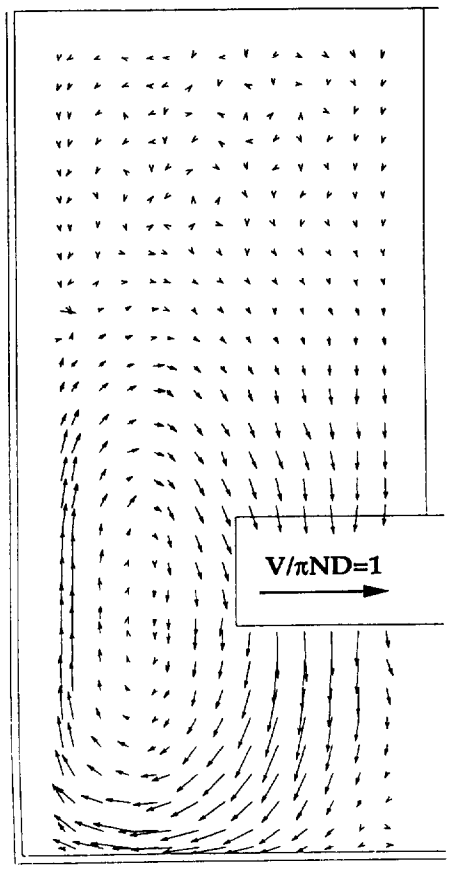

Fig. 5. Velocity field.

$$N_{Q_p} = Q_p / ND^3 \quad (7)$$

In order to determine the relative importance of the circulation flow in the tank compared with the discharge flow of the propeller, the circulation flow rate Q_c has been calculated at the level of the circulation loop, where r_c is the radial coordinate of the loop, i.e. at the point at which the sign of V_z is changing

$$Q_c = -2\pi \int_0^{rc} V_z \, r \, dr \quad (8)$$

and the non-dimensional circulation flow number N_{Q_c} is expressed by

$$N_{Q_c} = Q_c / ND^3 \quad (9)$$

Starting from the flow rate values obtained, two characteristic times can be calculated: the renewal time t_r

$$t_r = \text{Volume of the tank} / Q_p \quad (10)$$

and its non-dimensional value $t_r^* = Nt_r$; the circulation time t_c

$$t_c = \text{Volume} / Q_c \quad (11)$$

and its non-dimensional value $t_c^* = Nt_c$.

The axial velocities in the discharge flow of the Mixel TT propeller have been measured for two similar Reynolds numbers (10^5 and 1.25×10^5). The profiles, presented in Fig. 6, are very similar. In fact, in the range of Re corresponding to fully turbulent flows, the Reynolds number has no influence on the non-dimensional values of the velocity components [3] and, as a consequence, on the non-dimensional characteristic numbers of the propeller-tank system. For the Mixel TT propeller, a limit value of 10^5 for the Reynolds number above which the flow can be considered as fully turbulent has been determined by Pouzet et al. [28] by measuring the power consumption. Just below the shaft (near the axis of the vessel, $r/D > 0.1$), positive values of the axial component of the velocity (due to a slight vortex created by the shaft) can be seen. Such measurements very close to the axis have not been performed to establish the velocity field of the whole tank; as a consequence, these positive values of V_z cannot be observed in Fig. 6.

The non-dimensional values of the characteristic numbers of the system involved in this work are reported in Table 2.

Fig. 7 reports the tangential mean velocity profiles at four different levels in the vessel. In the upper part ($Z/D = 1.168$, for instance), the mean tangential component of the velocity

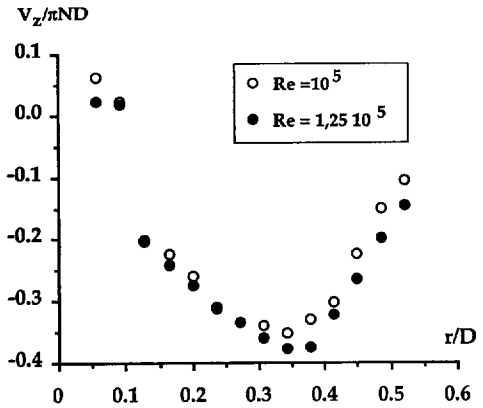

Fig. 6. Mean axial velocity profile in the discharge flow of the propeller.

Table 2
Characteristic numbers of the propeller–tank system

N_{Q_p}	N_{Q_c}	N_{Q_c}/N_{Q_p}	t_r^*	t_c^*
0.62	0.89	1.44	11.76	8.15

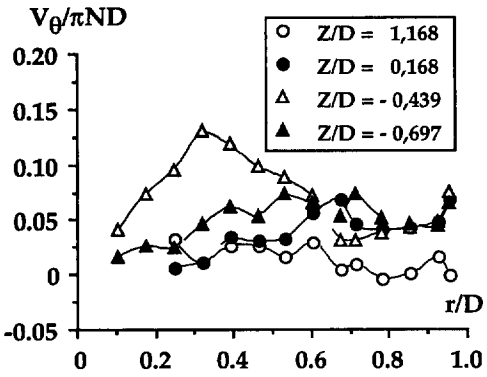

Fig. 7. Radial profiles of the mean tangential velocity.

remains lower than about 5% of the impeller tip velocity; the combination of an axial-type impeller and a fully baffled vessel avoids the appearance of a vortex (the Froude number, $Fr = N^2D/g$, is 0.37, but has no influence in this geometry).

Just above the impeller ($Z/D = 0.168$), this component is slightly more important near the wall; nevertheless, this small increase is not very significant. Under the impeller ($Z/D = -0.439$), the tangential velocity increases linearly from the axis of the vessel to a maximum value of about 15% of the impeller tip velocity, located at $r/D = 0.32$, the origin always being on the axis of the tank. The liquid just under the impeller seems to rotate, but with a lower angular velocity. For more important radial positions, the tangential velocities decrease under the action of the baffles. Near the bottom of the vessel ($Z/D = -0.697$), the tangential velocity remains lower than 8% of the impeller tip velocity and increases in the radial direction, with a constant angular velocity.

6. Two-phase flow measurements

Measurements have been performed in two-phase flow with the same flow conditions as in the case of the single-phase flow measurements. For each variable presented, three profiles are drawn:

1. the profile obtained in the absence of particles (liquid only);
2. the profile of the continuous phase (in the presence of particles);
3. the profile of the dispersed phase (particles).

6.1. Mean velocities

6.1.1. Mean axial velocities

Fig. 8(a)–8(f) show the axial profiles of the mean axial component of the velocity for six radial positions ($r/D = 0.179$, 0.321, 0.464, 0.679, 0.857 and 0.961 respectively).

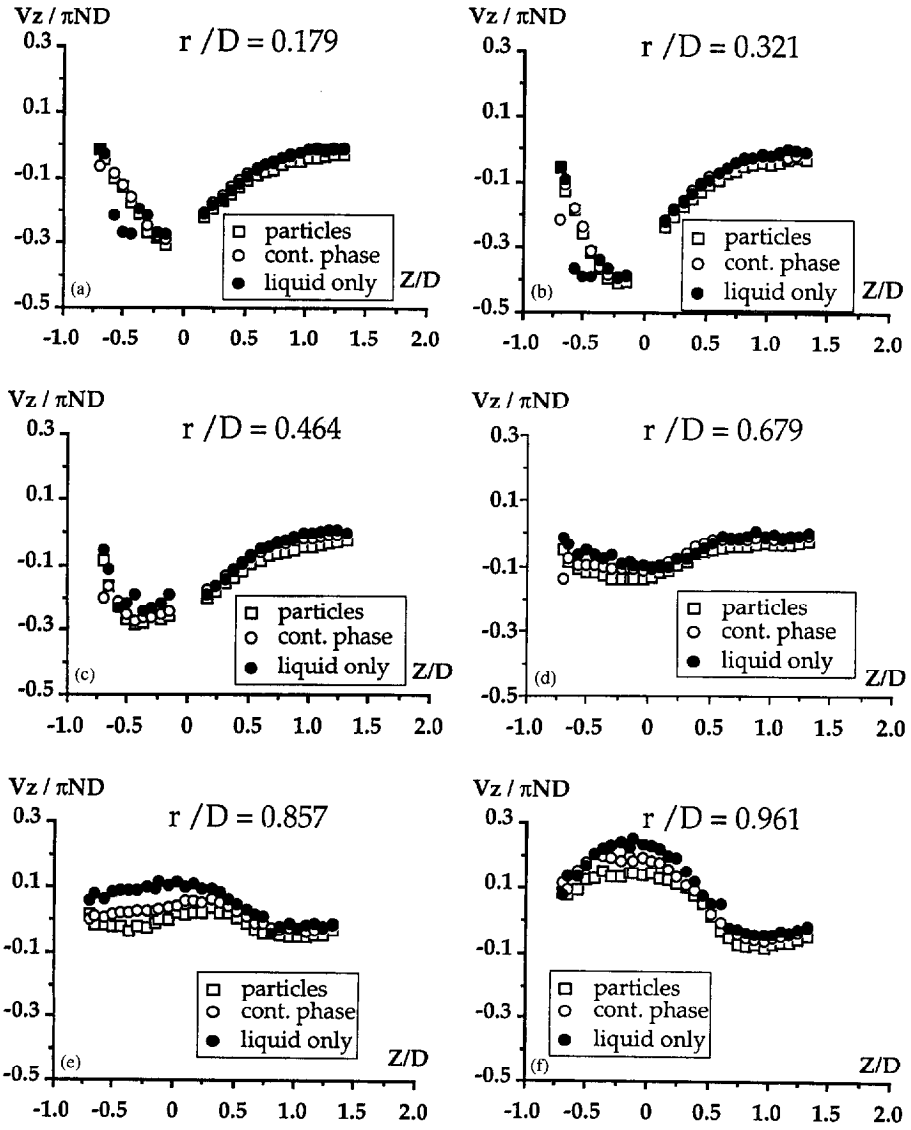

Fig. 8. Axial profiles of the mean axial velocity.

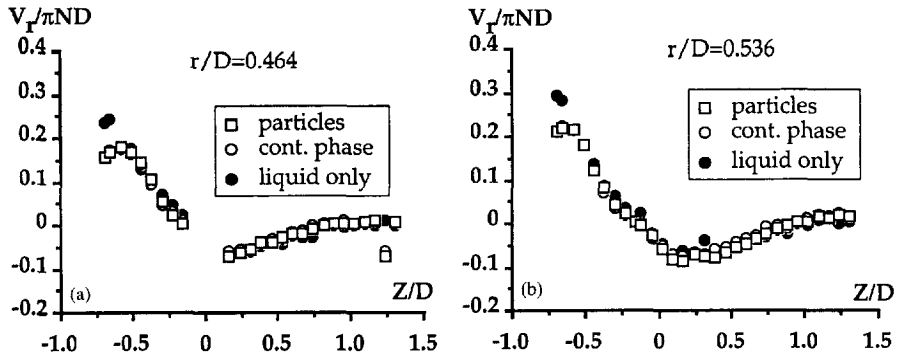

Fig. 9. Axial profiles of the mean radial velocity.

The whole set of measurements (not reported here) shows that, on the one hand, the flow behaviour is not really modified by the presence of particles at this very low volumetric concentration and, on the other, that the circulation pattern is similar for both phases.

A comparison between the profiles obtained for the continuous phase in the absence and presence of particles reveals that the liquid flow is disturbed by the solid in the discharge flow of the propeller (the slowing down is certainly due to the inertia of the glass particles, $r/D=0.179$, 0.321 and 0.464, $Z/D>0.5$) and near the wall of the vessel where the flow is moving upwards. In this part of the tank, the liquid is slowed down by the particles because of the effect of gravity. Solid particles are fluidized by the upward stream located along the wall of the vessel ($r/D=0.857$ and 0.961, $Z/D>0.5$). The glass particles lag behind the carrier phase in this part of the flow. In the downward parts of the flow field, the dispersed phase moves more quickly than the carrier fluid ($r/D=0.179$, 0.679 and 0.857), except for the discharge zone of the propeller where the velocities of both phases are equal.

6.1.2. Mean radial velocities

Fig. 9(a) and 9(b) show the axial profiles of the mean radial component of the velocity for two radial positions ($r/D=0.464$ and $r/D=0.536$ respectively). Only these two profiles are presented here because the mean radial velocities of the continuous and dispersed phases are identical with those obtained in the single-phase flow in the major part of the vessel. However, near the bottom, a slowing down can be observed, due to the presence of particles on the wall that must be rolled along the bottom by the carrier continuous phase. It should be noticed that the radial component of the slipping velocity between the particles and the liquid is not significant.

6.1.3. Mean tangential velocities

As mentioned for the single-phase flow measurements, the mean tangential velocity components are never important in the vessel. Fig. 10(a) and 10(b) show the axial profiles of this component at two radial positions ($r/D=0.464$ and $r/D=0.679$ respectively). As for the radial components, no significant tangential slip velocities appear in the vessel. It should be noted that the measurement of this velocity component is only possible, in the experimental apparatus used here, under the propeller if the sizes of the particles are determined at the same time.

6.2. Slip velocities

Fig. 11(a) and 11(b) give the axial profiles of the three components of the mean slip velocities at two radial positions in the vessel ($r/D=0.464$ and $r/D=0.679$ respectively). Similar results have been obtained at the other r/D values, but are not reported here. The axial component is more important than the other two components because the buoyancy force pulls the particles downwards.

The terminal velocity of the particles in the Stokes law region (V_{Ts}) and in the turbulent region (V_{Tt}) can be calculated using Eqs. (12) and (13) respectively

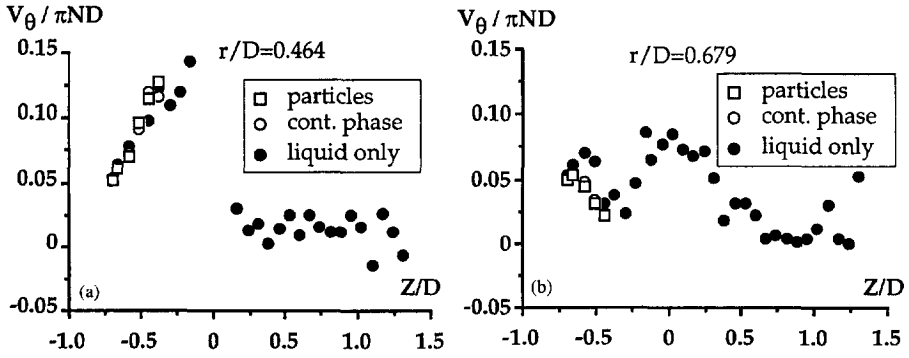

Fig. 10. Axial profiles of the mean tangential velocity.

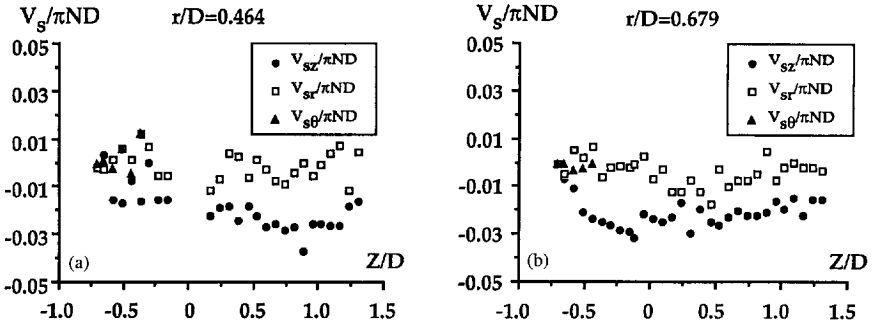

Fig. 11. Axial profiles of the slip velocities.

$$V_{Ts} = d^2(\rho_p - \rho)g/18\mu \quad (12)$$

$$V_{Tt} = \{4d(\rho_p - \rho)g/(3\rho C_d)\}^{1/2} \quad (13)$$

C_d is the drag coefficient and is taken as 0.44. With the same experimental conditions, the following values are obtained: $V_{Ts} = 43 \times 10^{-3}$ m s^{-1} and $V_{Tt} = 96 \times 10^{-3}$ m s^{-1}, or $V_{Ts}/V_t = 1.92 \times 10^{-2}$ and $V_{Tt}/V_t = 4.3 \times 10^{-2}$. The observed slip velocities are around this order of magnitude.

The slip velocity components are obtained from the difference between the velocities of the particles and the velocities of the continuous phase. Since these values are very similar, the addition of the measurement errors may be significant with regard to the resulting slip velocities. Moreover, it must be kept in mind that the local velocity measurements reported here are average values of the periodic and turbulent flow generated by the stirrer in the tank, and that the measurement technique used does not provide information about the local phase fraction. As a consequence, it is not easy to link the results obtained for the slip velocity components to the behaviour of the mean flow in the vessel, particularly to the mean vortex field. The flow seems to be too complex in a stirred tank to determine the effects that would be attributed to a lift force for example.

6.3. Root-mean-square velocities

6.3.1. Root-mean-square axial velocities

Fig. 12(a)–12(f) show the axial profiles of the root-mean-square axial component of the velocity for six radial positions ($r/D = 0.179$, 0.321, 0.464, 0.679, 0.857 and 0.929 respectively).

In the suction zone of the propeller, the root-mean-square axial velocity of the liquid is about 0.05 ($r/D = 0.179, 0.321$, 0.464; $Z/D < 0.2$). In the discharge flow, the root-mean-square axial velocities increase from the propeller to a maximum value (about 0.15) when the flow begins to return in order to slip along the bottom of the tank. Near the bottom, the root-mean-square axial velocities are smaller because the mean axial velocities decrease.

For a radius greater than the radius of the impeller ($r/D = 0.679$, for instance), the root-mean-square axial velocities decrease from about 0.12 near the bottom to 0.04 near the free surface of the liquid. It should be noticed that, just over the bottom, the values are always lower than a few centimetres above. In the upward stream located along the wall of the vessel ($r/D = 0.857$ and 0.929, $Z/D > 0.5$), the root-mean-square axial velocities increase slightly from the bottom to reach a maximum value for axial positions corresponding to the inversion of the axial mean velocity. For $Z/D < 0.5$, near the wall, the root-mean-square axial velocities decrease reaching about 0.04 near the surface.

A comparison between the profiles obtained for the continuous phase in the absence and presence of particles reveals that the fluctuations of the liquid are not disturbed by the dispersed phase in the major part of the vessel for this low volumetric concentration of particles. However, near the wall of the vessel, where the solid particles are fluidized by the upward stream ($r/D = 0.929$), a small increase in the axial fluctuations can be observed.

The root-mean-square axial velocities obtained for the particles are always greater than those measured for the continuous phase. The ratio between these components can reach two in some regions of the vessel. This effect is not obvious to explain. A reverse trend has been observed by Nouri and Whitelaw [16] in a vessel stirred by a Rushton-type impeller; however, a similar trend has been measured by Roco et al. [29] in a centrifugal pump. Several explanations can be proposed based on experimental or physical considerations.

The experimental velocities for the continuous and dispersed phases presented here have been obtained by modifying the intersection angle between the incident beams of the laser in order to change the size range of the measurements (a small angle in the case of the dispersed phase and a greater angle in the case of the continuous phase). Consequently, the measurement volume used to measure the velocity of the particles is larger than that used for the continuous phase. The particle velocity histogram may be enlarged by the spatial integration of the measurements over a larger measurement volume than in the case of the continuous phase, the root-mean-square value being increased as a consequence. The experimental technique used by Nouri and Whitelaw [16] can give a reverse trend: initially, they measured the single-phase velocity components; then, by reducing the photomultiplier sensitivity and partially closing an adjustable aperture placed in front of the photomultiplier, they eliminated the Doppler signals due to the fluid; they then inserted the dispersed phase in the vessel and measured the velocity components of the particles. This operating technique leads to a

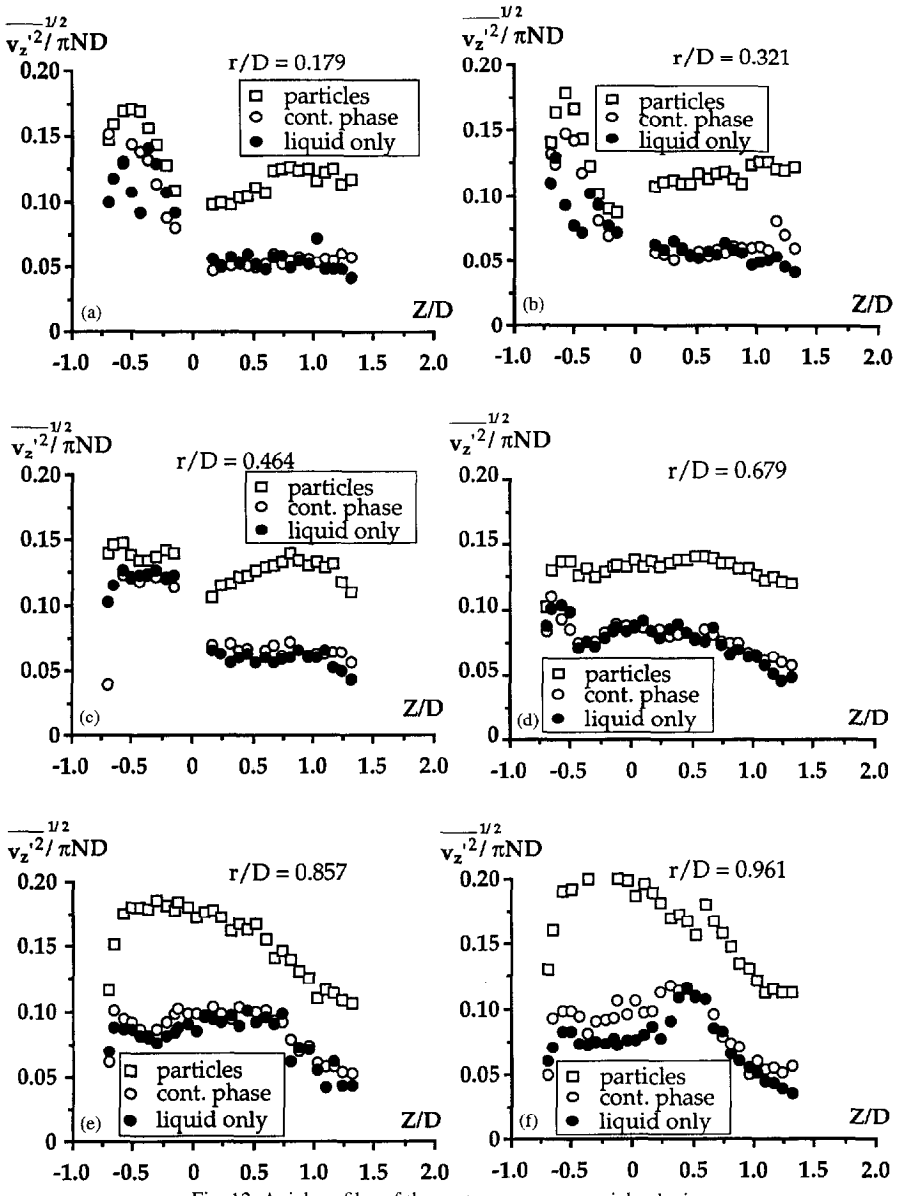

Fig. 12. Axial profiles of the root-mean-square axial velocity.

decrease in the real measurement volume, a narrowing of the particle velocity histogram and a reduction in the level of the root-mean-square velocity measured.

Physical reasons can also explain the root-mean-square axial velocity results: the dispersed phase used does not have a very narrow size distribution (165–350 μm, see Table 1); therefore the root-mean-square velocity of the particles can be partially due to a polydispersity effect. However, as shown in Fig. 13(a) and 13(b) (root-mean-square radial velocity), this effect is not observed on the other components of the root-mean-square velocity, probably because the buoyancy force does not act in these directions.

6.3.2. *Root-mean-square radial velocities*

The axial profiles of the root-mean-square radial velocities are shown in Fig. 13(a) and 13(b) for two radial positions ($r/D = 0.464$ and 0.536 respectively). In the suction zone of the propeller, the root-mean-square radial velocities are of the same order of magnitude as the axial ones. They increase from 0.05 near the surface of the suspension to reach 0.08 just above the propeller. In the discharge zone, the radial root-mean-square values initially decrease under the impeller, and then increase slightly just near the bottom wall, where the flow is diverted and transformed into a radial flow. For radial positions near the main circulation loop, and in the upward part of the flow, the radial velocity fluctuations are very similar to the axial ones. In this region, the root-mean-square values decrease from 0.1 near the bottom of the tank to about 0.05 near the surface.

As in the case of the axial root-mean-square components, the profiles obtained for the continuous phase in the presence of particles are very similar to those obtained in the absence of particles. However, unlike the observations made on the axial root-mean-square velocities, the profiles measured for

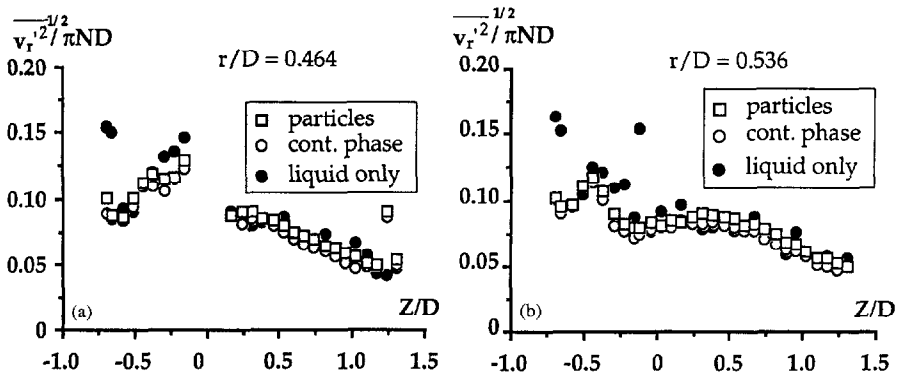

Fig. 13. Axial profiles of the root-mean-square radial velocity.

the radial root-mean-square velocities of the continuous phase and particles are very similar, a trend also noticed for the mean values of this velocity component.

6.3.3. Root-mean-square tangential velocities

The root-mean-square tangential velocities decrease slightly from 0.1 above the bottom of the vessel to about 0.05 just under the surface of the suspension. The three root-mean-square components of the velocity are similar in this upper part of the tank, where turbulence can be considered to be isotropic, as observed in other mixing tanks [3].

As in the case of the root-mean-square radial velocities, no significant differences can be observed between the measurements performed in the suspension for both phases and in the liquid without particles.

6.4. Field of mean diameter

At each measurement point, the size distribution of the particles passing through the measurement volume has been stored. In this temporal distribution, the number of particles in each size range depends on the velocity of the particles with this size. In order to obtain a spatial distribution, more representative of the size distribution at a point, the number of particles in each size range is weighted by the inverse of the mean velocity of this size range. A spatial mean diameter d can then be calculated by the relation [14]

$$d = \sum_{i=1}^{I} n_i d_i / \sum_{i=1}^{I} n_i \qquad (14)$$

where n_i is the 'weighted number' of particles in the size range of diameter d_i and I is the number of size ranges.

The measurements performed in the middle plane of the vessel are plotted in Fig. 14. The mean diameter is not constant over the vessel: the particles are larger in the regions of the tank external to the main circulation loop, especially in the corner made by the bottom and the wall, and at the top of the vessel. The larger particles are ejected by the centrifugal forces from the main circulation loop (see Fig. 5) where the vorticity is probably more important, and others are trapped by the dead zones where the vorticity level is lower. A suspension in a stirred tank cannot be assumed to be homogeneous, even when the rotation speed is higher than the critical speed to ensure the suspension.

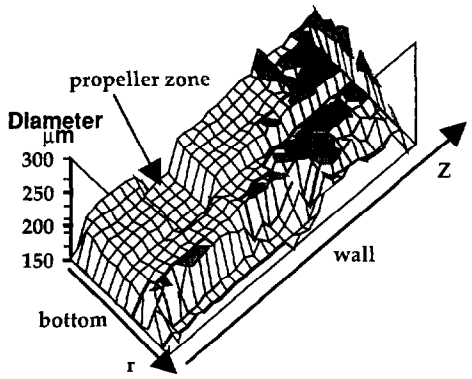

Fig. 14. Mean diameter field.

6.5. Influence of the particle size and stirring rate

Measurements of the axial velocity profiles have been performed at $r/D = 0.961$ for two samples of dispersed phase and four stirring rates (4.08, 5.10, 5.61 and 6.63 s^{-1} corresponding to Reynolds numbers of 8×10^4, 10^5, 1.1×10^5 and 1.3×10^5 respectively). The first sample is that used previously and the second, also spherical glass particles, has a greater mean size of 970 μm and a wider size distribution (between 630 and 1800 μm). The volumetric concentration of the particles in the suspension is 0.5%.

Fig. 15 summarizes the profiles obtained for the mean axial velocity of the particles along the axis of measurement. In

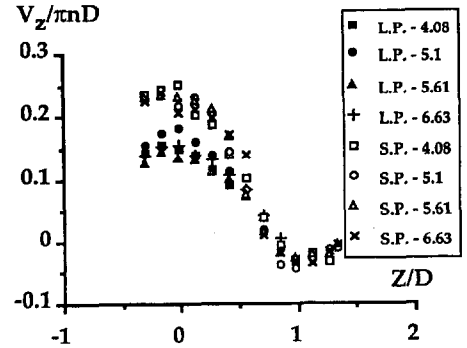

Fig. 15. Influence of the stirring rate and size range of the particles on the mean axial velocity of the particles.

the case of the larger particles (L.P.), no measurements are possible for Z/D greater than 0.9, because the amount of solid phase is not sufficient in this zone. In contrast, in the lower zone of the tank, the particle concentration is too important in the case of the larger particles to perform accurate measurements. The profile of the non-dimensional mean axial velocity of the dispersed phase is modified when the stirring rate is changed. Unlike the results usually obtained in single-phase agitated vessels [3], the circulation patterns of the dispersed phase in solid–liquid suspensions depend on the Reynolds number, even for high Re values.

The influence of the size of the particles is much more important. In the upward part of the flow field ($Z/D<0.6$), the fluidization of the largest particles is more difficult than that of the smallest; therefore their mean axial velocity is smaller, and their slip velocity is higher. The slip velocity has been evaluated for each size of particle at the axial position at which the axial velocity takes a maximum value and can be compared with the terminal velocity V_{Tt} calculated by Eq. (13). For the smaller particles ($d_p=253\times10^{-3}$ μm), the slip velocity V_s/V_t lies between 0.05 and 0.1; the value of V_{Tt}/V_t obtained from Eq. (13) is 0.043. For the larger particles, V_s/V_t lies in the range 0.23–0.28 and V_{Tt}/V_t, deduced from Eq. (13), is 0.19. The evolution in terms of the slip velocity follows that predicted by the terminal velocity correlation. The measured values are slightly lower, but this is not surprising in a turbulent flow.

7. Conclusions

The phase Doppler technique has been applied to the local measurement of the velocity and size of particles in a fully baffled vessel stirred by an industrial axial propeller at a low particle volumetric concentration of 0.5%. The spherical glass particles are suspended by water. The velocity measurements are treated in order to separate the data obtained for the smallest particles (representing the continuous water phase) and for the dispersed phase. Velocity measurements for a single-phase flow have permitted the calculation of the characteristic numbers of the tank–propeller system involved in this work. The mean velocity field reveals a main circulation loop developed by the propeller, and a minor contra-rotative circulation loop near the wall and the free surface.

Measurements in the two-phase liquid–solid system, with 253 μm mean diameter particles, show that the particles lag behind the continuous carrier phase in the upward parts of the flow field, but are ahead in some downward parts. The slip velocities are of the order of magnitude of the terminal velocity evaluated by classical correlations. The root-mean-square axial velocities obtained for the particles are always greater than those measured for the continuous phase. A mean diameter field over the plane of measurement has been provided and shows non-homogeneities in the suspension.

The effects of the stirring rate and size range of the particles have been determined in the upward part of the flow field. Even at high Reynolds numbers, the circulation patterns of the dispersed phase seem to be modified when the rotation speed is changed. Larger particles (970 μm) are more difficult to fluidize than smaller particles (253 μm) and have a lower mean axial velocity in the upward flow. The variation of the slip velocity with the size of the particles follows that predicted by the terminal velocity correlation in the turbulent region.

8. Nomenclature

b	function of the geometrical arrangement	m^{-2}
B_w	width of the baffles	m
C	impeller clearance	m
C_d	drag coefficient	–
d	diameter of the particles	m
D	diameter of the propeller	m
F_d	Doppler frequency	s^{-1}
g	acceleration due to gravity	ms^{-2}
h	height of the propeller	m
I	number of size ranges	–
n	number of particles	–
n_l	refractive index of the liquid phase	–
N	impeller rotation speed	s^{-1}
r	radial position	m
t_c	circulation time	s
t_r	renewal time	s
T	diameter of the vessel	m
V	velocity	$m\,s^{-1}$
v'	velocity fluctuation	$m\,s^{-1}$
V_{Ts}	terminal velocity in the Stokes law region	$m\,s^{-1}$
V_{Tt}	terminal velocity in the turbulent region	$m\,s^{-1}$
V_t	impeller tip velocity	$m\,s^{-1}$
Z	axial position	m

Greek letters

δ	fringe spacing	m
Δt	time difference between Doppler bursts	s
Φ	phase difference between Doppler bursts	rad
λ_0	wavelength of the laser beams	m
μ	dynamic viscosity	$kg\,m^{-1}\,s^{-1}$
ν	kinematic viscosity	$m^2\,s^{-1}$
ρ	density of the liquid	$kg\,m^{-3}$
ρ_p	density of the particles	$kg\,m^{-3}$
Ψ	off-axis angle	rad
θ	intersection angle of the laser beams	rad

Non-dimensional numbers

Fr	Froude number $=N^2D/g$	–
Re	Reynolds number of the stirred system $=ND^2/\nu$	–

N_{Qc}	non-dimensional circulation flow number $= Q_c/ND^3$	–
N_{Qp}	pumping coefficient $= Q_p/ND^3$	–
t_c^*	non-dimensional circulation time $= Nt_c$	–
t_r^*	non-dimensional renewal time $= Nt_r$	–

Subscripts

r	radial
S	slip
θ	tangential
z	axial

Acknowledgements

This work is supported by the Région Midi-Pyrénées, contract numbers RECH/9007906 and RECH/9200827.

References

[1] E.J. Lyons, in: V.W. Gray, J.B. Uhl (Eds.), Suspensions of solids, Mixing, Theory and Practice, UHL, Academic Press, New York, Chapter 9, 1967.

[2] M. Yianneskis, Z. Popiolek, J.H. Whitelaw, An experimental study of the steady and unsteady flow characteristics of stirred reactors, J. Fluid Mech. 175 (1987) 537–555.

[3] J. Costes, J.P. Couderc, Study by laser Doppler anemometry of the turbulent flow induced by a Rushton turbine in a stirred tank: Influence of the size of the units I: Mean flow and turbulence, Chem. Eng. Sci. 43 (1988) 2751–2764.

[4] M. Mahouast, G. Cognet, R. David, Two-component LDV measurements in a stirred tank, A.I.Ch.E. J. 35 (1989) 1770.

[5] H. Wu, G.K. Patterson, Laser Doppler Measurements of turbulent flow parameters in a stirred mixer, Chem. Eng. Sci. 44 (1989) 2207.

[6] V.V. Ranade, J.B. Joshi, Flow generated by pitched-blade turbines I: Measurements using laser Doppler anemometer, Chem. Eng. Comm. 81 (1989) 197.

[7] G.W. Smith, L.L. Tavlarides, J. Placek, Turbulent flow in stirred tanks: scale-up computations for vessel hydrodynamics, Chem. Eng. Comm. 93 (1990) 49–73.

[8] S.Y. Ju, T.M. Mulvahill, R.W. Pike, Three-dimensional turbulent flow in agitated vessels with a non-isotropic turbulence viscosity, Can. J. Chem. Engng. 68 (1990) 3–16.

[9] S.M. Kresta, P.E. Wood, Prediction of the three-dimensional turbulent flow in stirred tanks, A.I.Ch.E. J. 37 (1991) 3, 448–460.

[10] P. Ditl, Hydrodynamics and mass transfer in agitated suspensions, 5th European Conference on Mixing, Wurzburg (RFA) BHRA Cranfield, Bedford (England), 1985, pp. 179–189.

[11] J.B. Gray, J.Y. Oldshue, Agitation of particulate solid–liquid mixtures, in: V.W. Gray, J.B. Uhl (Eds.), Mixing – Theory and Practice, Academic Press, New York, Chapter 12, 1986.

[12] A. Barresi, G. Baldi, Solid dispersion in an agitated vessel, Chem. Eng. Sci. 42 (1987) 12, 2949–2956.

[13] P.A. Shamlou, E. Koutsakos, Solids suspension and distribution in liquids under turbulent agitation, Chem. Eng. Sci. 44 (1989) 3, 529–542.

[14] H. Yamazaki, K. Tojo, K. Miyanami, Effect of power consumption on solids concentration profiles in a slurry mixing tank, Powder Technol. 64 (1990) 199–206.

[15] R.K. Geisler, A.B. Mersmann, Local velocity distribution and power dissipation rate of suspensions in stirred vessels, 6th European Conference on Mixing, Pavia (Italy) BHRA Cranfield, Bedford (England) 1988, pp. 267–272.

[16] J.M. Nouri, J.H. Whitelaw, Particle velocity characteristics of dilute to moderately dense suspension flows in stirred reactors, Int. J. Multiphase Flow 18 (1992) 1, 21–23.

[17] M. Yianneskis, Velocity, particle sizing and concentration measurement techniques for multiphase flow, Powder Technol. 49 (1987) 261–269.

[18] H.A. Tsalapatas, M.L. Riethmuller, A real time personal computer-based clipped auto and cross correlator with applications in the detection of transition, 5th International Symposium on Application of Laser Techniques to Fluid Mechanics, Lisboa (Portugal), 1990.

[19] D.L. Reuss, R.J. Adrian, Two-dimensional velocity measurements in a laminar flame using Particle Image Velocimetry, Chem. Phys. Processes Combust. 11 (1988) 1–4.

[20] C.J.D. Pickering, N.A. Halliwell, Particle Image Velocimetry: data reduction and fringe analysis, 3rd International Symposium on Applications of Laser to Fluid Mechanics, Lisboa (Portugal), 1986.

[21] Y. Levy, LDA technique for measurement in freeboards of fluidized beds, A.I.Ch.E. J. 32 (1986) 9, 1579–1583.

[22] G. Grehan, G. Gouesbet, Corrected laser beam techniques for simultaneous velocimetry and sizing of particles in flow and applications, 3rd International Symposium on Applications of Laser to Fluid Mechanics, Lisboa (Portugal) 1986.

[23] F. Durst, M. Zare, Laser Doppler measurements in two-phase flows, LDA Symposium, Copenhagen (Denmark), 1975, pp. 403–429.

[24] W. Bachalo, M.J. Houser, Phase Doppler spray analyzer for simultaneous measurements of drop size and velocity distributions, Optical Engineering 23 (1984) 5, 583–590.

[25] K. Bauckage, H.M. Floegel, Simultaneous measurement of droplet size and velocity in nozzle sprays, 2nd International Symposium on Applications of Laser Anemometry to Fluid Mechanics, Lisboa (Portugal), 1984.

[26] M. Saffman, P. Buchhave, H. Tanger, Simultaneous measurement of size, concentration and velocity of spherical particles by a Laser Doppler Method, 2nd International Symposium on Applications of Laser Anemometry to Fluid Mechanics, Lisboa (Portugal), 1984.

[27] W.D. Bachalo, S.V. Sankar, Analysis of the light scattering interferometry for spheres larger than the light wavelength, 4th International Symposium on Applications of laser Anemometry to Fluid Mechanics, Lisboa (Portugal), 1986.

[28] S. Pouzet, C. Zuereb, G. Ranchin, Procédures expérimentales de caractérisation des performances d'un mobile d'agitation – application au cas d'hélices multiplans, Forum d'Agitation Industrielle, Toulouse (France) Récents Progrès en Génie des Procédés, 6, Agitation Industrielle, J. Bertrand, Lavoisier (Paris), 1993, pp. IV-47–IV-54.

[29] M.C. Roco, T. Cader, O. Masbernat, in: M.C. Roco, (Ed.), Periodic Liquid–solid Flow Microstructure in a Centrifugal Pump, Particulate Two-phase Flow, Butterworth–Heinemann, Chapter 13, 1992, pp. 391–437.